Med Chem Res
DOI 10.1007/s00044-012-0416-0

MEDICINAL CHEMISTRY RESEARCH

ORIGINAL RESEARCH

Benzothiazole Schiff-bases as potential imaging agents for β-amyloid plaques in Alzheimer's disease

Changsheng Gan · Lin Zhou · Zhenzhen Zhao · Haoshu Wang

Received: 1 June 2012 / Accepted: 11 December 2012

Abstract A series of benzothiazole Schiff-bases as potential diagnostic imaging agents targeting β-amyloid (Aβ) plaques in Alzheimer's disease (AD) were synthesized and evaluated. When in vitro binding studies using AD homogenate with [^{125}I] 6-iodo-2-(4′-dimethyl- amino)-phenyl-imidazo[1,2-α]pyridine ([^{125}I]IMPY) as the reference ligand were carried out with the derivatives, the compounds showed high to low binding affinities for AD homogenate at the K_i values ranged from 4.38 to 514.65 nM, depending on the substitution on the phenyl ring. Fluorescent staining in vitro showed that one compound with a *N*,*N*-dimethylamino group intensely stained Aβ plaques within brain sections of postmortem AD patients. The results strongly suggest that these derivatives are worthy of further study and may be a useful amyloid imaging agents for early detection of amyloid plaques in the brain of AD.

Keywords Alzheimer's disease · Amyloid plaques · Benzothiazole · Schiff-bases · Binding affinity

Introduction

Alzheimer's disease (AD) is a progressive neurodegenerative disorder and a leading cause of dementia (Selkoe, 2004; Querfurth and LaFerla, 2010; Nestor *et al*., 2004). Clinical symptoms of AD include cognitive decline, irreversible memory loss, disorientation, language impairment, etc. AD is characterized by abundant senile plaques (SPs) composed of β-amyloid (Aβ) peptides and neurofibrillary tangles (NFTs) formed from filaments of highly phosphorylated tau proteins (Nordberg, 2004, 2009). The amyloid cascade hypothesis indicates that the deposition of amyloid plaques constitutes a central and probably early event in the pathogenesis of AD. Therefore, the monitoring of Aβ plaques would be beneficial for the diagnosis, staging, and treatment of AD.

Presently non-invasively detection of Aβ plaques using PET and SPECT imaging tracers have been proposed as a useful tool for early diagnosis of AD. Several promising agents based on the backbone structure of Congo Red (CR), thioflavin-T (ThT), and DDNP labeled with ^{11}C, ^{18}F, ^{123}I have been synthesized and evaluated for in vivo imaging probes of Aβ plaques in AD brain (Mathis *et al*., 2004; Cai *et al*., 2007). In the last few years, clinical trials in AD patients have been reported with several agents including [^{11}C]-2-(4-(methylamino)phenyl)-6-hydroxybenzothiazole (PIB) (Mathis *et al*., 2003; Klunk *et al*., 2004), [^{11}C]-4-*N*-methylamino-4′-hydroxystilbene (SB-13) (Ono *et al*., 2003; Verhoeff *et al*., 2004), [^{18}F]-2-(1-(2-(*N*-(2-fluoroethyl)-*N*-methylamino)naphthalene-6-yl)ethylidene)-malononitrile (FDDNP) (Shoghi-Jadid *et al*., 2002), 6-iodo-2-(4′-dimethyl-amino)-phenyl-imidazo[1,2-α]pyridine (IMPY) (Zhuang *et al*., 2003; Newberg *et al*., 2006), [^{11}C]2-(2-(2-dimethylaminothiazol-5-yl)ethenyl) -6-(2-fluoroethoxy)benzoxazole (BF-227) (Kudo *et al*., 2007) (*E*)-4-(*N*-methylamino)-4′-(2-(2-(2-[^{18}F]fluoroethoxy)ethoxy)ethoxy)stilbene (BAY94-9172) (Rowe *et al*., 2008), ^{18}F-florbetapir ([^{18}F]AV-45) (Lin *et al*., 2010; Wong *et al*., 2010) and [^{18}F]3′-F-PIB (Nelissen *et al*., 2009) (Fig. 1), among which PIB is most widely studied and considered as one of the most promising probes in AD patients.

The above and other studies (Kung *et al*., 2001; Chandra *et al*., 2006; Duan and Liu, 2008; Nesterov *et al*., 2005) suggest some design rules of the amyloid probes that the molecule should be neutral and contain at least two aromatic

C. Gan (✉) · L. Zhou · Z. Zhao · H. Wang
Engineering Research Center of Bio-process of Ministry of Education, Hefei University of Technology, Hefei 230009, Anhui, People's Republic of China
e-mail: gancs7894@163.com

Published online: 20 December 2012

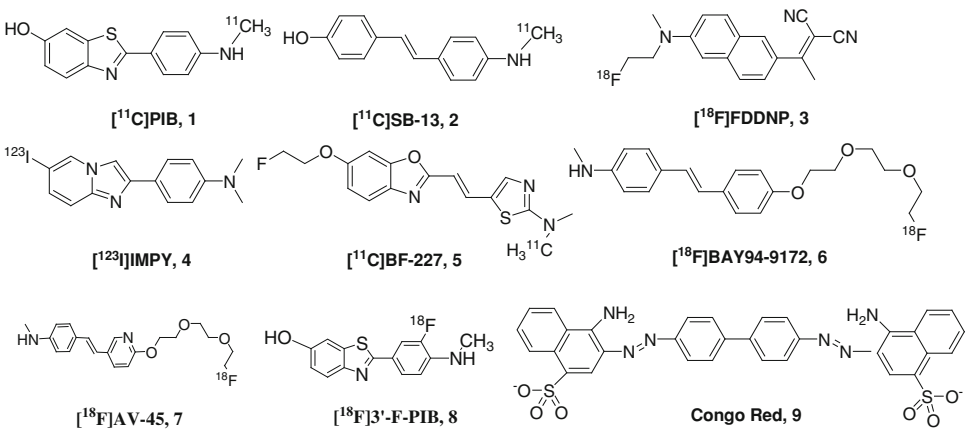

Fig. 1 Chemical structures of representative amyloid imaging agents

rings and a linker, and moreover, the presence of hydrophobic planarizable (or easily planarizable) conjugate system is an important design feature to obtain high binding affinity. The structure of stilbene is common in the reported imaging agents. In a previous literature (Lee *et al*., 2001), stilbene with double bond of C and C may isomerize in certain circumstance. Congo Red is one of the most frequently used imaging agents in the postmortem detection of AD patients, whose structure contains two double bonds of N and N. However, to our knowledge, Schiff-base with double bond of C and N is scarcely reported as the amyloid imaging agent. In this article, we designed a novel series of benzothiazole Schiff-bases (compound **12** in Scheme 1) with the key structure or pharmacophore of PIB and double bond of C and N as the linker. The compounds were synthesized and evaluated with postmortem AD homogenate. Compounds **12a** and **12c** exhibited high binding properties, which can be further radiolabeled by C-11 or F-18 to be used for in vivo imaging of amyloid plaques in AD (Manook *et al*., 2012; Neumaier *et al*., 2010; Yousefi *et al*., 2011).

Results and discussion

Chemistry

The synthesis of the benzothiazole Schiff-bases is outlined in Scheme 1. The target compounds were easily prepared by direct condensation of benzothiazole with different benzaldehyde under the catalysis of acidic catalyst. By screening the catalyst, acetic acid, *p*-toluenesulfonic acid, and other Lewis acids, such as anhydrous $ZnCl_2$, we selected HOAc as the appropriate catalyst. The reaction could be smoothly carried out under equivalent HOAc in reflux EtOH with different substrates.

Biological evaluation

In vitro binding assay

The binding affinities (K_i) of the benzothiazole Schiff-bases were evaluated by radioligand competition binding assay with [^{125}I]IMPY for Aβ plaques using homogenates prepared from postmortem AD brain tissues. [^{125}I]IMPY was prepared as described previously (Zhuang *et al*., 2003). The results are shown in Table 1.

The binding properties changed greatly while the substituents varied. In the case of **12b**, where the phenyl rings carry strongly electron-withdrawing NO_2 groups (R = NO_2), the K_i was found to be 514.65 nM. However, the replacement of the NO_2 groups with NMe_2 (compound **12a**) or OMe (compound **12c**) resulted in a steep decrease in the K_i value (4.38 and 10.82 nM, respectively). It proves that the phenyl rings should be electron rich in order for these compounds to exhibit high binding affinities. For compounds **12d** and **12e**, when substituent R is changed from Br to I, only low

Scheme 1 Synthesis of benzothiazole Schiff-bases

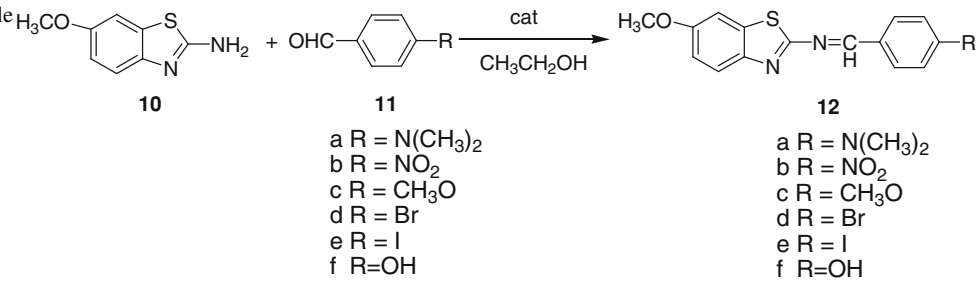

Table 1 Inhibition constants (K_i) of compound **12** on ligand binding to AD brain homogenates

Entry	Compounds	K_i (nM)
1	**12a**	4.38 ± 0.41
2	**12b**	514.65 ± 53.37
3	**12c**	10.82 ± 1.30
4	**12d**	106.46 ± 8.63
5	**12e**	102.74 ± 6.88
6	**12f**	34.72 ± 2.87
IMPY		5.30 ± 0.36

Values are the mean for three independent experiments

binding affinities were obtained with insignificant difference. Compound **12f** with substituent R as OH also showed a good binding property with K_i value of 34.72 nM.

Combined with the previous reports (Carter and Chou, 1998; Klunk *et al*., 1999), some clues can be inferred from the results. The binding affinity is largely due to the hydrogen bond, hydrophobic interaction, π–π stacking, and electrostatic interaction between the ligand and the target protein. All the investigated compounds bearing benzothiazole and phenyl ring can form π–π stacking or hydrophobic interaction with the amyloid peptides. Compounds **12a**, **12c**, and **12f** exhibited higher binding properties, probably because of its substituents, which can form hydrogen bond with the amyloid aggregates more easily. The structure bearing electron-rich aromatic rings is more favorable for binding properties possibly owing to the stronger interaction of π–π stacking.

AD brain tissue fluorescent staining

As these benzothiazole derivatives could emit fluorescence well, the AD brain tissue fluorescent staining was further performed for visually investigating the binding ability of these compounds to the SPs in vitro. As shown in Fig. 2, almost all the SPs in the brain section were labeled by ligand **12a** (B1), as confirmed by staining with thioflavin S (ThS, A1) in the adjacent section as compared to the blank control section (C1). Details of SP staining could be clearly visualized by the fluorescence of **12a** (B2), while the staining pictures in the red rectangle were expanded as shown in the bottom row of Fig. 2. Hollow arrow refers to the SPs. Interestingly, similar to ThS (A2), the NFTs, as indicated by triangle arrows in Fig. 2, could also be labeled by **12a** (B2). The binding properties of both amyloid plaques and tangles as FDDNP suggest it may be potentially helpful in the diagnosis of Alzheimer's disease and mild cognitive impairment (Petersen *et al*., 2006; Guillozet *et al*., 2003; Small *et al*., 2006; Barrio *et al*., 2008; Shin *et al*., 2008).

Experimental section

Materials and instruments

The reagents used in the syntheses were purchased from Alfa Aesar, Sigma-Aldrich and Sinopharm Chemical Reagent Co. Ltd and were used without further purification unless otherwise indicated. The AD human brain homogenates and paraffin brain sections were obtained from the Netherlands brain bank (coordinator: Dr. I. Huitinga). The ^{1}H NMR spectra were obtained on a Bruker Avance-500 (500 MHz) spectrometer with TMS as the internal standard. FT-IR spectra were obtained on a Thermo Scientific Nicolet 8700 system.

General procedure for the preparation of the benzothiazole Schiff-bases

To a mixture of 2-amino-5-methoxybenzothiazole (1 mmol) and different substituted benzaldehyde (1 mmol) in 10 mL of anhydrous ethanol was added to acetic acid (1 mmol) dropwise. The reaction mixture was refluxed for 18 h. After cooling to room temperature, the precipitate was filtered to give an orange (**12a**, **12b**) or yellow solid (**12c**–**12f**), which was purified by silica gel chromatography to give the desired products (**12a**–**12f**).

12a

^{1}H-NMR (300 MHz, $CDCl_3$) δ 8.80 (s, 1H), 7.88 (d, 2H, J = 9.0 Hz), 7.80 (d, 1H, J = 8.9 Hz), 7.27 (d, 1H, J = 2.6 Hz), 7.03 (dd, 1H, J = 2.6, 8.9 Hz), 6.73 (d, 2H, J = 9.0 Hz), 3.88 (s, 3H), 3.10 (s, 6H). IR (cm^{-1}) 3033, 2938, 2832, 1603, 1577, 1471, 1230, 1167, 1061, 839.

12b

^{1}H-NMR (300 MHz, $CDCl_3$) δ 9.15 (s, 1H), 8.36 (d, 2H, J = 8.8 Hz), 8.19 (d, 2H, J = 8.8 Hz), 7.90 (d, 1H, J = 9.0 Hz), 7.33 (d, 1H, J = 2.5 Hz), 7.12 (dd, 1H, J = 2.5, 9.0 Hz), 3.91 (s, 3H). IR (cm^{-1}) 3066, 2941, 2836, 1601, 1558, 1513, 1483, 1342, 1220, 844.

12c

^{1}H-NMR (300 MHz, $CDCl_3$) δ 8.92 (s, 1H), 7.97 (d, 2H, J = 8.8 Hz), 7.84 (d, 1H, J = 8.9 Hz), 7.29 (d, 1H, J = 2.6 Hz), 7.06 (dd, 1H, J = 2.6, 8.9 Hz), 7.01 (d, 2H, J = 8.8 Hz), 3.90 (s, 3H), 3.89 (s, 3H). IR (cm^{-1}) 3006, 2965, 2934, 1603, 1565, 1424, 1262, 1145, 1051, 1022, 838.

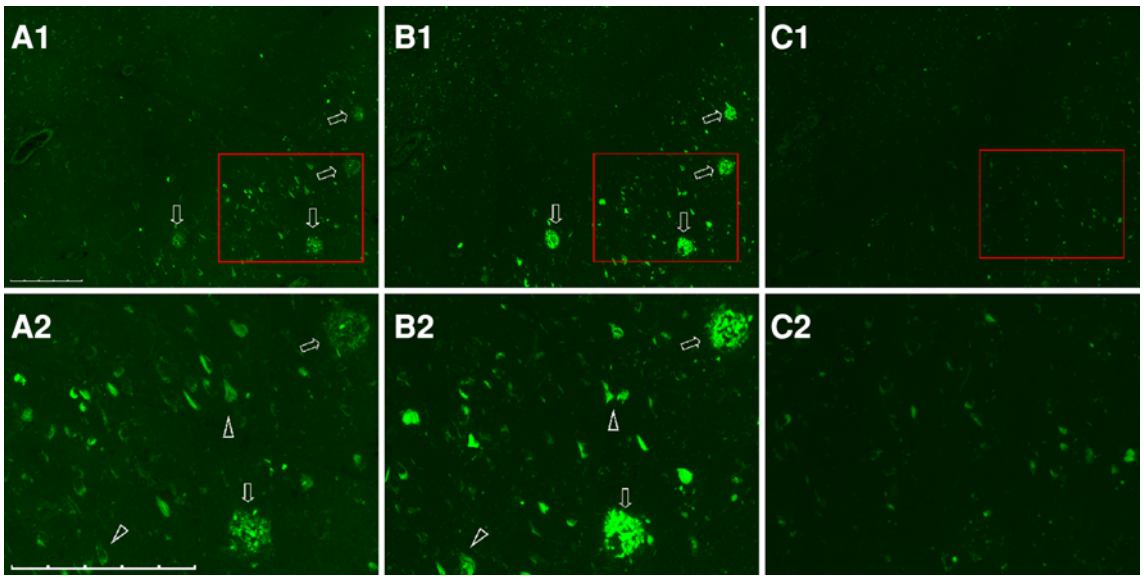

Fig. 2 Three adjacent AD brain sections were stained (**a** ThS, **b 12a**, **c** blank control). The *hollow arrows* indicate the amyloid plaques. The *triangle arrows* indicate the neurofibrillary tangles. The *bottom row* was the magnified images of the *boxed area* in the *top row*. *Bar* 250 μm (Color figure online)

12d

^{1}H-NMR (300 MHz, $CDCl_3$) δ 8.97 (s, 1H), 7.87 (m, 3H), 7.66–7.64 (m, 2H), 7.30 (m, 1H), 7.10–7.07 (m, 1H), 3.89 (s, 3H). IR (cm^{-1}) 3013, 2968, 2940, 1602, 1586, 1484, 1267, 1228, 1057, 847.

12e

^{1}H-NMR (300 MHz, $CDCl_3$) δ 8.96 (s, 1H), 7.89–7.86 (m, 3H), 7.72 (d, 2H, $J = 8.3$ Hz), 7.30 (d, 1H, $J = 2.3$ Hz), 7.08 (dd, 1H, $J = 2.3$, 8.9 Hz), 3.89 (s, 3H). IR (cm^{-1}) 3073, 2936, 2829, 1614, 1555, 1495, 1264, 1224, 1054, 865.

12f

^{1}H-NMR (300 MHz, $CDCl_3$) δ 8.98 (s, 1H), 7.94 (d, 2H, $J = 8.6$ Hz), 7.79 (d, 1H, $J = 8.9$ Hz), 7.63 (d, 1H, $J = 2.4$ Hz), 7.10 (dd, 1H, $J = 2.4$, 8.9 Hz), 6.96 (d, 2H, $J = 8.6$ Hz), 3.85 (s, 3H). IR (cm^{-1}) 3033, 2939, 1603, 1578, 1523, 1471, 1269, 1230, 1167, 839.

Preparation of brain tissue homogenates

Frozen AD brain tissues were thawed and placed on ice. The gray and white matters were dissected, weighed, and homogenized in ice-cooled phosphate buffered saline (PBS) solution (0.05 M, pH 7.4) at a concentration of approximately 100-mg wet tissue/mL using a motor-driven homogenizer (Glas-Col, USA). The homogenates were aliquoted into 1-mL portions and stored at −80 °C. For binding assays, the homogenates were thawed, diluted with ice-cold PBS solution (0.05 M, pH 7.4), and homogenized again using an ice-cold hand-held glass homogenizer.

In vitro binding assays with AD brain homogenates

Radioligand competition binding assays were carried out in 12 × 75 mm borosilicate glass tubes. To a glass tube AD brain homogenates (100 μL), 0.05 nM radioligand [^{125}I]IMPY (100 μL), inhibitor (100 μL, 3×10^{-6} to 1×10^{-10} M), and 0.05 M PBS (pH 7.4, 700 μL) were added to bring the final volume to 1 mL. Non-specific binding was defined in the presence of 600-nM IMPY in the same assay tubes. The mixture was incubated at 37 °C for 2 h, and the bound and the free radioactivity were separated by vacuum filtration through Whatman GF/B filters using a ZT-II-12R cell harvester followed by 2 × 3 mL washes of PBS at room temperature. Filters containing the bound I-125 ligand were counted in a gamma counter (USTC Zonkia GC-1200, Hefei, China) with a 65 % counting efficiency. Values for the half-maximal inhibition concentration (IC_{50}) were computed from displacement curves of three independent experiments using GraphPad Prism 5. In addition, the inhibition constant (K_i) was calculated using the Cheng–Prusoff equation: $K_i = IC_{50}/(1 + [L]/K_d)$, where [L] is the concentration of radioligand used in the assay, and K_d is the dissociation constant of radioligand.

AD brain tissue fluorescent staining

Brain tissues were obtained from autopsy-confirmed AD subjects. Adjacent tissue sections (6 μm thickness) were processed for staining. First, the paraffin brain sections were treated with 2 × 10 min washes in xylene, 2 × 10 min washes in 100 % ethanol, 5-min sequential washes in 95, 90, 80, and 70 % ethanol, and sequential rinsings (5 min each) in milli-Q water and phosphate buffered saline (0.01 M PBS, pH 7.4). Second, to quench the autofluorescence, the sections were blanched in 0.25 % potassium permanganate solution for 20 min, washed in PBS, and treated with 0.1 % potassium metabisulfite and 0.1 % oxalic acid in PBS, followed by washing in PBS. Quenched brain tissue sections were immersed in the solution of a cold ligand (50 μM in 30 % EtOH/PBS, 20 min), ThS (1 % in milli-Q water, 5 min). Third, the sections were differentiated by 50 % EtOH/H_2O for 10 min (cold ligand), or 70 % EtOH/H_2O for 10 min (ThS). Finally, the sections were washed in PBS (3 × 5 min) and sealed by 80 % glycerin/PBS and cover-slips. These sections were stored at 4 °C in darkness and viewed using an Olympus IX71 fluorescence microscope (Olympus, Tokyo) with an SPOT digital camera (Diagnostic Instruments, Detroit, MI).

Conclusions

A series of benzothiazole Schiff-bases were readily prepared and compounds **12a**, **12c**, **12f** exhibited high binding affinities to amyloid plaques in AD brain. These derivatives with high affinities provide the possibility of a scaffold for potential molecular imaging agents to monitor Aβ plaques in the brain of AD patients.

Acknowledgments We are grateful to the Key Laboratory of Brain Function and Disease, Chinese Academy of Sciences for financial support.

References

Barrio JR, Kepe V, Satyamurthy N, Huang SC, Small G (2008) Amyloid and tau imaging, neuronal losses and function in mild cognitive impairment. J Nutr Health Aging 12:61S–65S

Cai L, Innis RB, Pike VW (2007) Radioligand development for PET imaging of beta-amyloid (Abeta)—current status. Curr Med Chem 14:19–52

Carter DB, Chou KC (1998) A model for structure-dependent binding of Congo red to Alzheimer beta-amyloid fibrils. Neurobiol Aging 19:37–40

Chandra R, Kung MP, Kung HF (2006) Design, synthesis, and structure-activity relationship of novel thiophene derivatives for beta-amyloid plaque imaging. Bioorg Med Chem Lett 16:1350–1352

Duan XH, Liu BL (2008) Aβ-binding molecules: possible application as imaging probes and as anti-aggregation agents. Sci China B 51:801–807

Guillozet AL, Weintraub S, Mash DC, Mesulam MM (2003) Neurofibrillary tangles, amyloid, and memory in aging and mild cognitive impairment. Arch Neurol 60:729–736

Klunk WE, Jacob RF, Mason RP (1999) Quantifying amyloid β-peptide (Aβ) aggregation using the Congo red-Aβ (CR-Aβ) spectrophotometric assay. Anal Biochem 266:66–76

Klunk WE, Engler H, Nordberg A, Wang Y, Blomqvist G, Holt DP, Bergstrom M, Savitcheva I, Huang GF, Estrada S, Ausen B, Debnath ML, Barletta J, Price JC, Sandell J, Lopresti BJ, Wall A, Koivisto P, Antoni G, Mathis CA, Langstrom B (2004) Imaging brain amyloid in Alzheimer's disease with Pittsburgh Compound-B. Ann Neurol 55:306–319

Kudo Y, Okamura N, Furumoto S, Tashiro M, Furukawa K, Maruyama M, Itoh M, Iwata R, Yanai K, Arai H (2007) 2-(2-[2-Dimethylaminothiazol-5-yl]ethenyl)-6-(2-[fluoro]ethoxy)benzoxazole: a novel PET agent for in vivo detection of dense amyloid plaques in Alzheimer's disease patients. J Nucl Med 48:553–561

Kung HF, Lee CW, Zhuang ZP, Kung MP, Hou C, Plössl K (2001) Novel stilbenes as probes for amyloid plaques. J Am Chem Soc 123:12740–12741

Lee CW, Zhuang ZP, Kung MP, Plössl K, Skovronsky D, Gur T, Hou C, Trojanowski JQ, Lee VM, Kung HF (2001) Isomerization of (Z, Z) to (E, E)1-bromo-2,5-bis-(3-hydroxycarbonyl-4-hydroxy)-styrylbenzene in strong base: probes for amyloid plaques in the brain. J Med Chem 44:2270–2275

Lin KJ, Hsu WC, Hsiao IT, Wey SP, Jin LW, Skovronsky D, Wai YY, Chang HP, Lo CW, Yao CH, Yen TC, Kung MP (2010) Whole-body biodistribution and brain PET imaging with [^{18}F]AV-45, a novel amyloid imaging agent—a pilot study. Nucl Med Biol 37:497–508

Manook A, Yousefi BH, Willuweit A, Platzer S, Reder S et al (2012) Small-animal PET imaging of amyloid-beta plaques with [^{11}C]PiB and its multi-modal validation in an APP/PS1 mouse model of Alzheimer's disease. PLoS ONE 7(3):e31310. doi: 10.1371/journal.pone.0031310

Mathis CA, Wang Y, Holt DP, Huang GF, Debnath ML, Klunk WE (2003) Synthesis and evaluation of ^{11}C-labeled 6-substituted 2-arylbenzothiazoles as amyloid imaging agents. J Med Chem 46:2740–2754

Mathis CA, Wang Y, Klunk WE (2004) Imaging beta-amyloid plaques and neurofibrillary tangles in the aging human brain. Curr Pharm Des 10:1469–1492

Nelissen N, Van Laere K, Thurfjell L, Owenius R, Vandenbulck M, Koole M, Bormans G, Brooks DJ, Vandenberghe R (2009) Phase 1 study of the Pittsburgh Compound B derivative ^{18}F-flutemetamol in healthy volunteers and patients with probable Alzheimer disease. J Nucl Med 50:1251–1259

Nesterov EE, Skoch J, Hyman BT, Klunk WE, Bacskai BJ, Swager TM (2005) In vivo optical imaging of amyloid aggregates in brain: design of fluorescent markers. Angew Chem Int Ed Engl 44:5452–5456

Nestor PJ, Scheltens P, Hodges JR (2004) Advances in the early detection of Alzheimer's disease. Nat Med 10:S34–S41

Neumaier B, Deisenhofer S, Sommer C, Solbach C, Reske SN, Mottaghy F (2010) Synthesis and evaluation of ^{18}F-fluoroethylated benzothiazole derivatives for in vivo imaging of amyloid plaques in Alzheimer's disease. Appl Radiat Isot 68(6):1066–1072

Newberg AB, Wintering NA, Plössl K, Hochold J, Stabin MG, Watson M, Skovronsky D, Clark CM, Kung MP, Kung HF (2006) Safety, biodistribution, and dosimetry of ^{123}I-IMPY: a novel amyloid plaque-imaging agent for the diagnosis of Alzheimer's disease. J Nucl Med 47:748–754

Nordberg A (2004) PET imaging of amyloid in Alzheimer's disease. Lancet Neurol 3:519–527

Nordberg A (2009) The future: new methods of imaging exploration in Alzheimer's disease. Front Neurol Neurosci 24:47–53

Ono M, Wilson A, Nobrega J, Westaway D, Verhoeff P, Zhuang ZP, Kung MP, Kung HF (2003) ^{11}C-labeled stilbene derivatives as Abeta-aggregate-specific PET imaging agents for Alzheimer's disease. Nucl Med Biol 30:565–571

Petersen RC, Parisi JE, Dickson DW, Johnson KA, Knopman DS, Boeve BF, Jicha GA, Ivnik RJ, Smith GE, Tangalos EG, Braak H, Kokmen E (2006) Neuropathologic features of amnestic mild cognitive impairment. Arch Neurol 63:665–672

Querfurth HW, LaFerla FM (2010) Mechanisms of disease: Alzheimer's disease. N Engl J Med 362:329–344

Rowe CC, Ackerman U, Browne W, Mulligan R, Pike KL, O'Keefe G, Tochon-Danguy H, Chan G, Berlangieri SU, Jones G, Dickinson-Rowe KL, Kung HP, Zhang W, Kung MP, Skovronsky D, Dyrks T, Holl G, Krause S, Friebe M, Lehman L, Lindemann S, Dinkelborg LM, Masters CL, Villemagne VL (2008) Imaging of amyloid beta in Alzheimer's disease with ^{18}F-BAY94-9172, a novel PET tracer: proof of mechanism. Lancet Neurol 7:129–135

Selkoe DJ (2004) Alzheimer disease: mechanistic understanding predicts novel therapies. Ann Intern Med 140:627–638

Shin J, Lee SY, Kim SH, Kim YB, Cho SJ (2008) Multitracer PET imaging of amyloid plaques and neurofibrillary tangles in Alzheimer's disease. Neuroimage 43:236–244

Shoghi-Jadid K, Small GW, Agdeppa ED, Kepe V, Ercoli LM, Siddarth P, Read S, Satyamurthy N, Petric A, Huang SC, Barrio JR (2002) Localization of neurofibrillary tangles and beta-amyloid plaques in the brains of living patients with Alzheimer disease. Am J Geriatr Psychiatry 10:24–35

Small GW, Kepe V, Ercoli LM, Siddarth P, Bookheimer SY, Miller KJ, Lavretsky H, Burggren AC, Cole GM, Vinters HV, Thompson PM, Huang SC, Satyamurthy N, Phelps ME, Barrio JR (2006) PET of brain amyloid and tau in mild cognitive impairment. N Engl J Med 355:2652–2663

Verhoeff NP, Wilson AA, Takeshita S, Trop L, Hussey D, Singh K, Kung HF, Kung MP, Houle S (2004) In-vivo imaging of Alzheimer disease beta-amyloid with [^{11}C]SB-13 PET. Am J Geriatr Psychiatry 12:584–595

Wong DF, Rosenberg PB, Zhou Y, Kumar A, Raymont V, Ravert HT, Dannals RF, Nandi A, Brasic JR, Hilton J, Lyketsos C, Kung HF, Joshi AD, Skovronsky DM, Pontecorvo MJ (2010) *In vivo* imaging of amyloid deposition in Alzheimer disease using the radioligand ^{18}F-AV-45 (florbetapir F 18). J Nucl Med 51: 913–920

Yousefi BH, Drzezga A, von Reutern B, Manook A, Schwaiger M, Wester HJ, Henriksen G (2011) A novel ^{18}F-labeled imidazo[2,1-*b*]benzothiazole (IBT) for high-contrast PET imaging of β-amyloid plaques. ACS Med Chem Lett 2(9):673–677

Zhuang ZP, Kung MP, Wilson A, Lee CW, Plössl K, Hou C, Holtzman DM, Kung HF (2003) Structure-activity relationship of imidazo[1,2-a]pyridines as ligands for detecting beta-amyloid plaques in the brain. J Med Chem 46:237–243